Dealkalization of Bauxite residue through Acid Neutralization and its Revegetation Potential

Hua Zeng[1], Fei Lyu[2], Guangyan Hu[3], Honghu Tang[4], Li Wang[5], Wei Sun[6], Yuehua Hu[7], Runqing Liu[8], Pan Chen[9]
1. Postgraduate Student of School of Minerals Processing and Bioengineering
2. PhD Student of School of Minerals Processing and Bioengineering
3. Postgraduate Student of School of Minerals Processing and Bioengineering
4. Lecturer of School of Minerals Processing and Bioengineering
5. Associate professor of School of Minerals Processing and Bioengineering
6. Dean of School of Minerals Processing and Bioengineering
7. Executive Vice President of Central South University
8. Associate professor of School of Minerals Processing and Bioengineering
9. Associate professor of School of Minerals Processing and Bioengineering
Central South University, Changsha 410083, China;
Corresponding author: sunmenghu@csu.edu.cn

Abstract

Bauxite residue is an alkaline industrial solid waste generated in alumina production process and the high alkalinity has caused serious environmental pollution. In this paper, a fast, high efficiency and low cost de-alkali process was developed, of which bauxite residue was dealkalized by sulfuric acid and calcium-containing compound CAM. And the revegetation potential of de-alkali bauxite residue was also studied. The results showed that the de-alkali rate reached up to 94.31 % when added 18.4 % of sulfuric acid and 2 % of CAM leaching at room temperature for 10 - 30 min. And the filtration speed increased by about 70 times with the addition of CAM up to 4.5 %. Subsequent pot experiment showed that the de-alkali bauxite residue met the growth requirements of plants. SEM analysis showed that the particle size of neutralized bauxite residue was enlarged, accelerating the process of soil formation of bauxite residue. This work provided technical support for ecological restoration of bauxite residue disposal area.

Keywords: bauxite residue; dealkalization; acid neutralization; revegetation; ecological restoration.

1. Introduction

Bauxite residue is an alkaline industrial solid waste generated in alumina production process [1]. Depending on bauxite type, 1 - 1.5 t of bauxite residue is produced when generating 1 t of alumina production [2]. The total amount of bauxite residue globally was about 160 Mt in 2015 [3]. Due to its abundant bauxite resources [4], China has become the largest producer of bauxite residue. The total bauxite residue production of China in 2016 was about 88 Mt [3]. As of 2017, the global reserves of bauxite residue have reached 3.9×10^3 Mt [5], of which China has accumulated more than 350 Mt [6]. However, the average utilization factor of global bauxite residue is only 15 %, and that of China is only 4 % [7].

The traditional disposal method of bauxite residue is building a dam in the open [8]. However, the cost of bauxite residue damming is very high, accounting for about 2 % of the price of alumina [9]. The fine size and strong alkalinity of bauxite residue caused serious air pollution [10], land pollution and water pollution [9]. Owing to the potential environmental risks of the large-scale pile-up of bauxite residue, researches on the ecological restoration of bauxite residue have been conducted worldwide. At present, gypsum [11] and organic matter (e.g., composts, manures, bio solids) [11b] are often used as amendments for the ecological restoration of bauxite residue.

Moreover, bauxite residue contains large amounts of Al, Fe, Ti, and other valuable components [12], all belonging to potential secondary solid resources. Several researchers have extensively investigated the comprehensive utilization of bauxite residue. Bauxite residue are mainly used in the (1) preparation of building materials, such as bricks [13], cement [14] and concretes [15], subgrade materials [16], and ceramics [17]; (2) preparation of adsorbent materials [18] for wastewater processing; and (3) extraction of valuable metals, including aluminum [19], titanium [20], iron [21], gallium [22], and scandium [23].

Among these different uses, making building materials can consume a large amount of bauxite residue [24] and produce lower environmental pollution [3], thus using bauxite residue in building materials is an important means of using it on a large scale. And the sodium content in the raw materials for preparing building materials require to be less than 0.5 %, which prevent the occurrence of "efflorescence" phenomenon affecting production quality [25]. However the sodium content in bauxite residue is 2 % - 10 % [12], which is much higher than the requirements of building materials and the standard salt content of the soil (high salinity soil, salt content > 0.4 % [26]). Thus, sodium in bauxite residue cannot be used directly by soil or to make construction materials. So the dealkalization of bauxite residue is the key factor for its comprehensive utilization.

The conventional methods of bauxite residue dealkalization are water leaching, acid leaching, calcium ion replacement, and wet carbonization [7, 27]. The water leaching method can remove free alkali in bauxite residue and has no agent consumption, but it requires several times of dealkalization and long-term leaching, prolonging the operation time and affecting the subsequent comprehensive utilization of bauxite residue. Acid leaching can significantly improve the de-alkali rate of bauxite residue, but the acid consumption is extremely large in the de-alkali process. After de-alkali, the acidity of bauxite residue are so strong that it is not conducive to dam stacking or to the preparation of building materials and other comprehensive use. Calcium ion replacement method can significantly remove free alkali and structural alkali in bauxite residue, but its agents consumption is larger and de-alkali rate is generally less than 80 %. Wet carbonization can effectively remove free alkali and structural alkali in bauxite residue with no agent consumption, but leaching equipment requirements are more stringent, leaching process conditions are difficult to control and operation is more cumbersome.

In the process of direct acid neutralization, silicon in bauxite residue is easily immersed to form silica gel, seriously affecting the filtration performance of bauxite residue [28]. Additionally, this gelatinous precipitate may blind ore particles from further dissolution and reduce the leaching kinetics significantly [28], making solid-liquid separation harder.

In this paper, a fast, high-efficiency, low-cost de-alkali process of bauxite residue was proposed, which was dealkalized by sulfuric acid and calcium-containing compound CAM. Then the revegetation potential of de-alkali bauxite residue was studied. The flowsheet of bauxite residue treatment is shown in Figure 1.

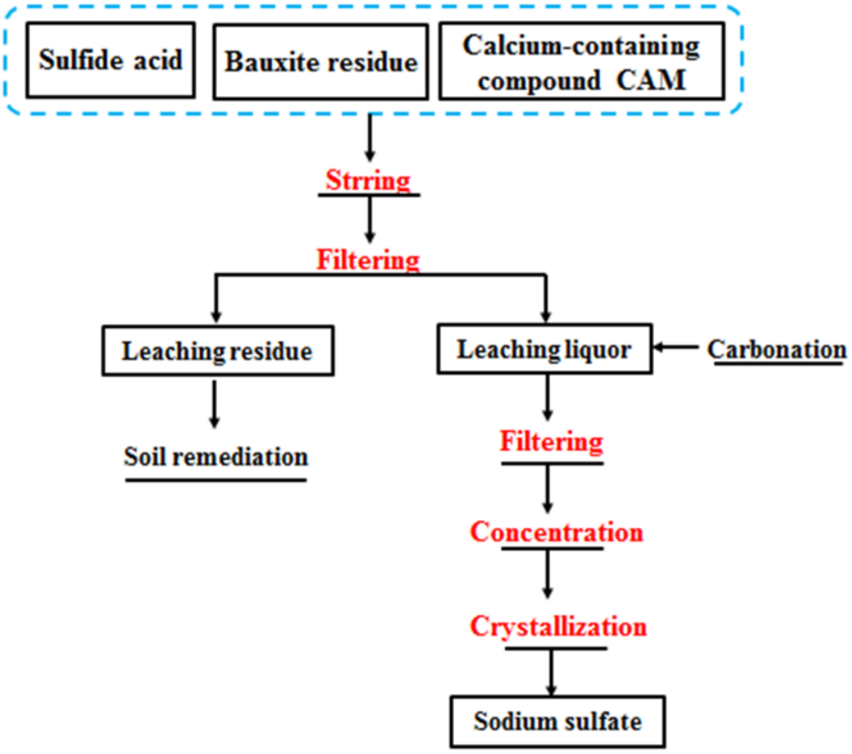

Figure 1. Flowsheet of bauxite residue treatment.

2. Materials and Methods

2.1. Materials

The test bauxite residue was derived from a Bayer Process alumina plant in Shandong Province. Table 1 showed the main chemical composition of the bauxite residue. The bauxite residue is mainly composed of Al, Fe, Si, Na, and Ca elements, and Na_2O content is as high as 9.79 %. If not treated with it, the bauxite residue will cause serious environmental pollution and cannot be used for secondary resources.

Table 1. Major chemical compositions of bauxite residue.

Element	Al_2O_3	CaO	Fe_2O_3	TiO_2	Na_2O	SiO_2
Content/%	20.57	2.10	23.17	5.77	9.79	15.10

The main mineral phase of bauxite residue was analyzed by an inductively coupled atomic (XRD, D8 Advance, BRUKER). Figure 2 showed the XRD pattern of bauxite residue. As can be seen from the figure, the main mineral phase of the bauxite residue is gibbsite, anatase, hematite, limonite, calcite, and quartz and sodium is mainly stored in complex aluminosilicates.

Analytical purity reagents and deionized water were used throughout the tests.

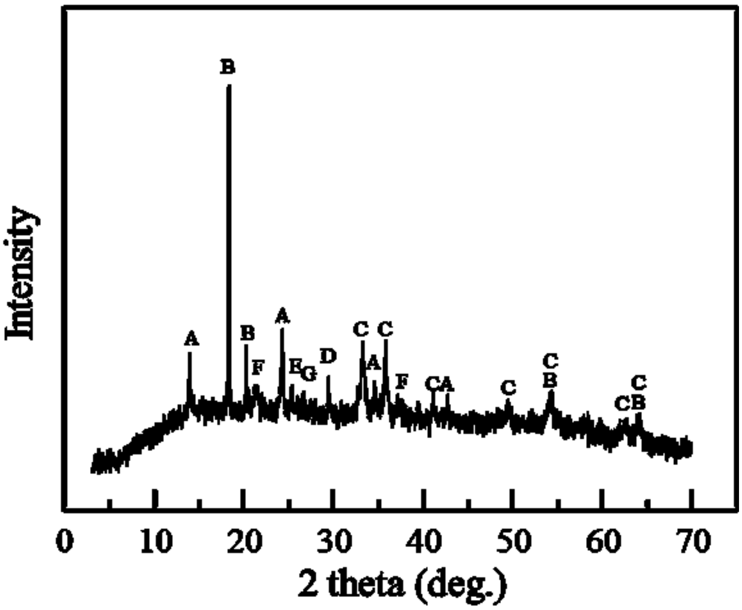

Figure 2. XRD pattern of bauxite residue.

A, $1.08Na_2O{\bullet}Al_2O_3{\bullet}1.68SiO_2{\bullet}1.8H_2O$; B, gibbsite; C, hematite; D, calcite; E, anatase; F, limonite; G, quartz.

2.2. Methods

2.2.1. Dealkalization Test

Different dosages and types of acid were used for acid neutralization, which was performed on the magnetic mixer and leached at room temperature for 10 - 30 min with liquid to solid ratio of 2:1. At the end of the experiment, the bauxite residue was filtered to separate leaching residue and leachate. The leaching residue was dried, digested, and then the Na^+ content was measured with an inductively coupled atomic emission spectrometer (ICP-OES, SPECTRO BLUE SOP, SPECTRO). According to formula (1), de-alkali rate can be calculated.

$$\varepsilon = \frac{m_0C_0 - m_1C_1}{m_0C_0} \times 100\% \tag{1}$$

Where ε is de-alkali rate, %; C_0 is the content of Na^+ in original bauxite residue, %, C_1 is the content of Na^+ in de-alkali bauxite residue, %, m_0 is the weight of original bauxite residue, g, and m_1 is the weight of de-alkali bauxite residue, g.

XRF analysis of leaching residue and leachate was carried out for the analysis of the de-alkali effect of bauxite residue, using an X-ray fluorescence analyzer (XRF, PANalytical Axios mAX, PANalytical B.V.). The microstructure of bauxite residue before and after alkali removal was observed with a scanning electron microscopy (SEM, Phenom ProX, Phenom Scientific). Particle size of bauxite residue before and after de-alkali was measured by a laser particle size analyzer (Mastersizer 2000, Malvern).

2.2.2. Revegetation Test

Pot experiments were carried out in original bauxite residue (OBR), sulfuric acid neutralized bauxite residue (SBR), 2 % of CAM modified bauxite residue (CBR), and bauxite residue neutralized by sulfuric acid and 2 % of CAM (SCBR), respectively. Ryegrass was selected as potted plants with a seeding depth of about 2 cm. After sowing 50 seeds, the soil was compacted slightly and watered to the maximum water holding rate of 60 % - 70 %. After 20 days, germination rate was counted and calculated. After sowing for 50 days, the whole plant above the surface was cut, washed, and dried. The average plant height and the average wet weight of the whole plant were measured. Then, the strains were placed in an oven and dried at 105 °C for the measurement of the average dry weight of the whole plant. The bulk density of the substrates was determined by the cutting ring method. The electrical conductivity (EC) of the substrates was measured with a DDS-307a conductivity meter, the pH value of the substrates was determined with a PHS-25 type acidity meter, and the density of the substrates was determined by the pycnometer method.

3. Results and Discussions

3.1. Acid Neutralization

Figure 3 showed the effect of different types and dosages of acid on the de-alkali rate of bauxite residue. The de-alkali rate of bauxite residue increased gradually with the dosage of acid, and sulfuric acid showed the best. With the increase of H^+ concentration up to 1.84 mol/L, the de-alkali rate of sulfuric acid reached up to 91.06 %, which was 75.12 % higher than that of nothing addition. The de-alkali rate of sulfuric acid was also 10.36 % and 56.52 % higher than that of the same H^+ concentration of hydrochloric acid and phosphoric acid, respectively, while that of oxalic acid was between that of hydrochloric acid and phosphoric acid. Moreover, sulfuric acid is widely available and has a low price, so it is recommended for the dealkalization of bauxite residue.

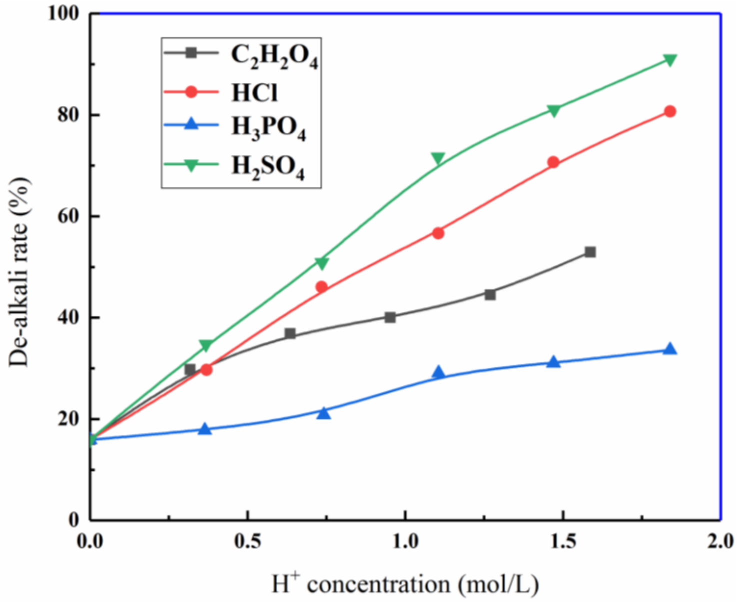

Figure 3. Effect of acid on de-alkali rate of bauxite residue.

3.2. Effect of CAM on Acid Neutralization

In the process of direct acid neutralization, silicon in bauxite residue is partially dissolved, and silica gel and other substances are formed, which seriously affect the filtration performance of bauxite residue [28]. In this paper, calcium-containing compound CAM was added through acid neutralization and the relationship between CAM and filtration performance was investigated. Two experiments were designed as follows: (1) the sulfuric acid de-alkali test as the first group was carried out with 18.4 % (relative to the amount of bauxite residue) of sulfuric acid and (2) combined de-alkali test as the second group was carried out with 18.4 % of sulfuric acid and 2 %

of CAM. Figure 3 showed the effect of the two groups on the de-alkali rate of bauxite residue and the relationship between CAM usage and filtration performance.

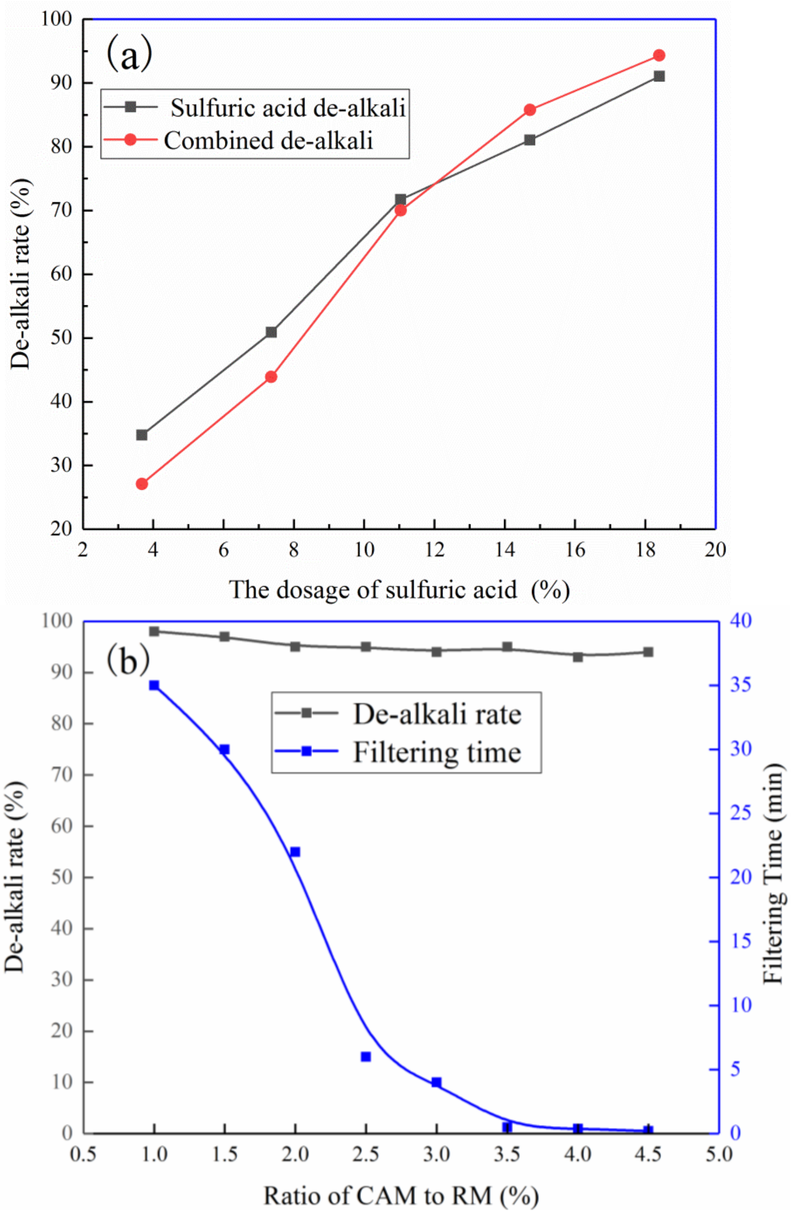

Figure 4. (a) Effect of sulfuric acid dosage (relative to the amount of bauxite residue) on de-alkali rate of bauxite residue; (b) Relationship between filtration performance and CAM dosage.

As shown in Figure 4(a), the de-alkali rate of second group reached up to 94.31 %, which was 3.25 % higher than that of first group. When the dosage of sulfuric acid is low, the de-alkali rate of the two groups is similar. When the amount of sulfuric acid was at higher level, the de-alkali rate of the second group was slightly higher than that of the first group. The possible reason was that the free alkali and amorphous sodium aluminosilicate were completely removed, and excess sulfuric acid destroyed the structure of the bauxite residue structure alkali with Ca^{2+} replaced Na^{+}, causing higher de-alkali rate [29]. As shown in Figure 4(b), with the increase in CAM usage from 1 % to 4.5 %, the filtration time was reduced from 35 min to 0.2 min, the filtration speed increased by about 70 times and de-alkali rate was almost constant. It is probably because that the fine-grain silica gel was captured to generate precipitation, which made solid-liquid separation easier. It can be concluded that CAM greatly improved the filtration performance of acid neutralization without any adverse effects on alkali removal from bauxite residue.

3.3. Effect of CAM on Aggregate Structure

The particle size distribution of original bauxite residue, sulfuric acid de-alkali bauxite residue and combined de-alkali bauxite residue was measured, respectively. The results was listed in Table 2 and depicted in Figure 5.

Table 2. Particle size distribution of original bauxite residue, sulfuric acid de-alkali bauxite residue and combined de-alkali bauxite residue.

Particle size(μm)	Original bauxite residue (%)	Sulfuric acid de-alkali bauxite residue (%)	Combined de-alkali bauxite residue (%)
<0.01	0	0	0
0.01- 0.1	11.02	3.51	0
0.1 - 1	49.53	14.54	0
1 - 10	19.97	11.34	10.47
10 - 100	17.66	37.12	55.37
100 - 1000	1.79	33.49	33.80

It can be seen that the grain level of bauxite residue before and after de-alkali has greatly changed. The particle size of the original bauxite residue was mainly concentrated in 0.1- 10 μm and 0.01-0.1 μm accounted for a maximum of 49.53 %. The particle size of sulfuric acid de-alkali bauxite residue was mainly concentrated in 10 -1000 μm, of which 10 - 100 μm accounted for a maximum of 37.12 %. The particle size of combined de-alkali bauxite residue was mainly concentrated in 10 - 1000 μm and 10 - 100 μm accounted for a maximum of 55.73 %. The grain level of sulfuric acid de-alkali bauxite residue was coarser than that of the original bauxite residue, showing that sulfuric acid de-alkali can promote the reunion between bauxite residue particles. And the grain level of combined de-alkali was coarser than that of sulfuric acid de-alkali bauxite residue, indicating that combined de-alkali can further accelerate the reunion between bauxite residue particles.

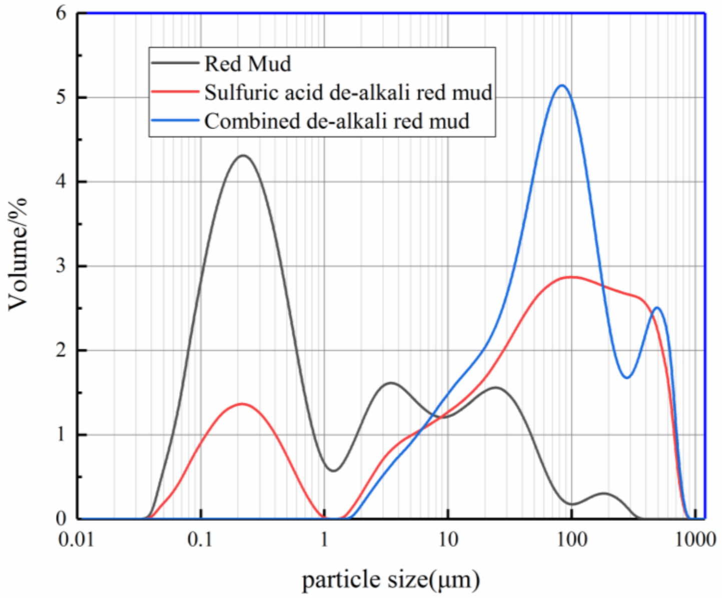

Figure 5. Particle size distribution of bauxite residue.

3.4. Effect of CAM on Leaching Residue and Leachate

XRF analysis was carried out on the original bauxite residue and the combined de-alkali bauxite residue. Table 3 showed the chemical composition of bauxite residue before and after de-alkali. The sodium residue of bauxite residue decreased from 11.709 % to 0.302 % and proved that most of alkali in bauxite residue was removed. The chemical composition of other elements before and after de-alkali changed little, which indicated that the dealkalization of bauxite residue would not affect other elements. It also showed that the leachate after de-alkalization was simple and can be used to make high pure sodium products for the subsequent process.

Table 3. Chemical composition of bauxite residue before and after de-alkali.

Element	Bauxite residue (%)	Combined de-alkali bauxite residue (%)	Element	Bauxite residue (%)	Combined de-alkali bauxite residue (%)
O	36.956	37.58	K	0.083	0.048
Na	11.709	0.302	Ca	1.332	0.829
Mg	0.096	0.085	Ti	4.398	5.525
Al	11.025	12.22	Cr	0.078	0.08
Si	8.143	6.691	Mn	0.064	0.086
p	0.095	0.126	Fe	25.483	33.828
S	0.259	0.126	Zn	0.008	0.009

The results of the all-element analysis of leachate are in Table 4. It was found that large amounts of Al, Si, Mg, and other elements remained in the sulfuric acid de-alkali leachate, while these elements in the combined de-alkali leachate were close to 0, indicating the composition of the combined de-alkali leachate was simple. It can be concluded that the addition of CAM inhibited the dissolution of Al, Si, Mg, and other elements, and simplified the follow-up treatment of leachate.

Table 4. Chemical composition of leachate.

Element	Sulfuric acid de-alkali leachate (mg/L)	Combined de-alkali leachate (mg/L)	Element	Sulfuric acid de-alkali leachate (mg/L)	Combined de-alkali leachate (mg/L)
Al	1631	0.6	Mg	60	5
B	1	0.3	Mn	5	0.3
Ca	459	433	Na	14130	13830
Co	0.2	0.04	Nd	1	0.03
Cr	0.2	0.06	Ni	0.4	0.1
Cu	0.8	0.1	P	1	0.04
Fe	0.4	0.07	Pb	0.2	0.03
K	77	108	S	12900	9970
Li	0.2	0.1	Si	664	32
V	0.2	0.07	Y	1	0.01

3.5. SEM Analysis

The morphology of OBR, SBR and SCBR was analyzed by SEM at different magnifying rates (5000×, 10,000×; Figure 6). As shown in Figure 6, the particle size of aggregates increased significantly in the following order: OBR < SBR < SCBR, which increased from several microns to dozens microns. It indicated that both sulfuric acid and CAM could promote the reunion of bauxite residue particles and the two substances showed synergistic effect. It is conducive to subsequent ecological remediation, or application in other industrial activities.

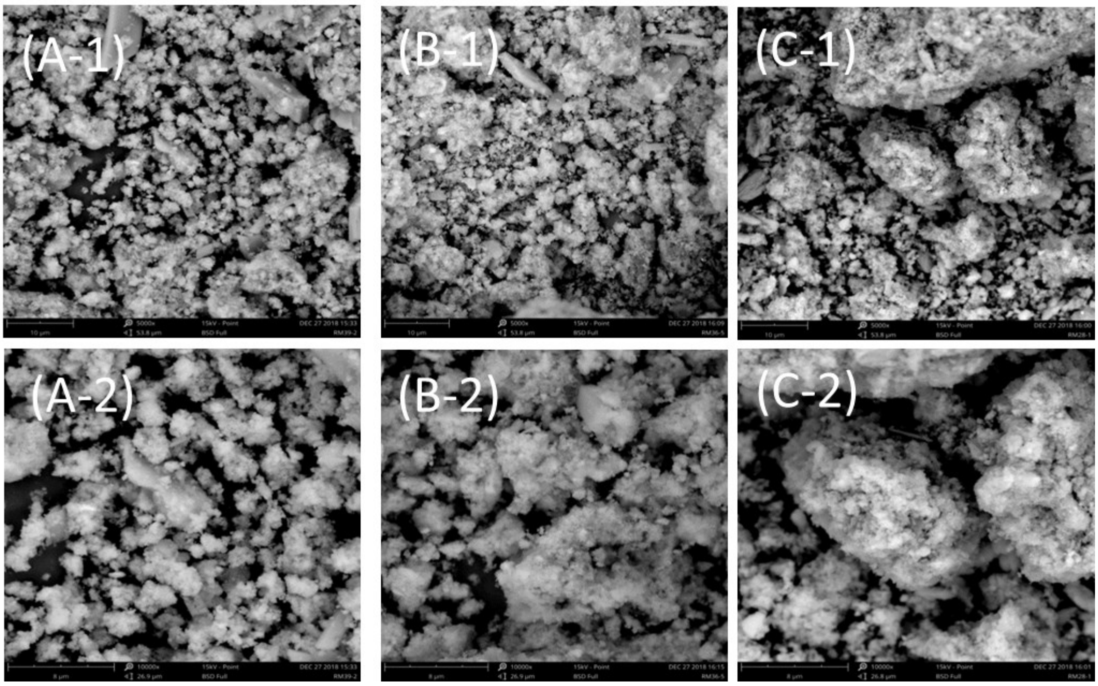

Figure 6. SEM images of (A) original bauxite residue, (B) sulfuric acid de-alkali bauxite residue and (C) combined de-alkali bauxite residue. (A-1), (B-1), (C-1):5000 times; (A-2), (B-2), (C-2):10000 times.

3.6. Revegetation Potential

Figure 7 shows the growth performance of the ryegrass planted on soil and four groups of substrates. OBR and CBR could not meet the requirement of the growth of ryegrass, and resulting in blank data. The germination rate of ryegrass grown on SBR was 86 % and that grown on SCBR increased to 92 %. The germination rates of both groups reached to the basic requirements of plant cultivation. Compared with the average height of 25.97 cm, wet weight of 0.29 g and dry weight of 0.066 g of soil-grown ryegrass, the average plant height and wet weight of ryegrass grown on SCBR was 31.03 % and 13.96 % higher while that of ryegrass grown on SBR was 6.35% and 0.24 % lower, indicating that the neutralized residue generally met the requirements of ryegrass growth. Nevertheless, the dry weight of ryegrass grown on SBR and SCBR was 16.7 % and 3.76 % lower than that grown on soil, indicating the less organics accumulation in ryegrass as a result of the lack of nutrition in bauxite residue. Therefore, it is necessary to introduce organic fertilizer in bauxite residue disposal area during ecological restoration.

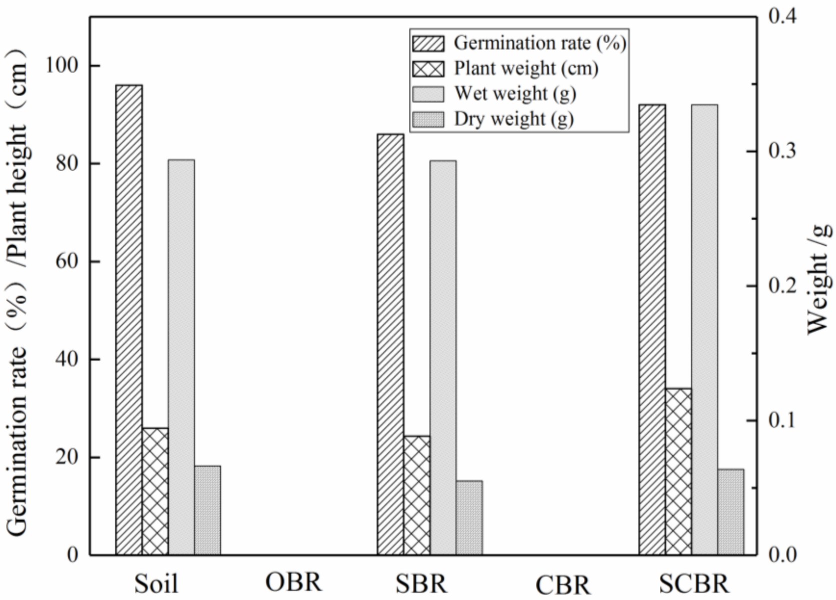

Figure 7. Growth performance of ryegrass grown on different substrates.

Table 5 shows the basic properties of the four groups of substrates after reclamation. Bulk density, pH and electrical conductivity (EC) are basic indexes that reflect whether the soil is suitable for plant growth. According to previous literature, the bulk density should be reduced to less than 1.6 g/cm^3, pH should below 9.0 but above 5.5 and EC should be less than 4 mS/cm [11b]. The pH of OBR and CBR were 10.84 and 10.34, respectively, which were not satisfied for plant growth. However, the pH of SBR and SCBR decreased to 6 - 7, meeting the basic requirements of plant growth. Density and bulk density reflect the porosity of the substrates. By comparison, the density and bulk density of SCBR were smaller than those of SBR, showing that the SCBR substrates was loose, porous, and beneficial to the growth of ryegrass. EC reflects the content of ions in the substrates, and soluble salt content in the substrates increased with conductivity. In the four groups of substrates, SCBR had the lowest conductivity and thus the lowest soluble salt content. It can concluded that the combined de-alkali bauxite residue was a suitable substrate for plant growth.

Table 5. Properties of different substrates.

Properties	pH	EC (mS/cm)	Density (g/cm^3)	Bulk density (g/cm^3)
Original Bauxite residue (OBR)	10.84	3.52	2.917	1.26
Sulfuric acid de-alkali bauxite residue (SBR)	7.31	5.07	3.117	1.20
CAM improved bauxite residue (CBR)	10.34	3.58	3.573	1.58
Combined de-alkali bauxite residue (SCBR)	6.79	3.40	3.105	1.13

4. Conclusions

Bauxite residue is an alkaline industrial solid waste generated in alumina production process and the high alkalinity has caused serious air pollution, land pollution and water pollution. Acid neutralization is an effective method to remove alkali from bauxite residue, but the low filtration efficiency restricts its application. In this paper, a fast, high efficiency and low cost de-alkali process was developed, of which bauxite residue was dealkalized by sulfuric acid and calcium-containing compound CAM. The revegetation potential of the neutralized residue has also been studied. The main conclusions were drawn as follows:

1) De-alkali rate of bauxite residue could reached up to 94.16 % with 18.4 % of sulfuric acid and 2 % of CAM addition at room temperature for 10 - 30 min; with higher addition rate of CAM, the filtration speed increased by about 70 times without adverse effects on de-alkali rate;
2) SEM analysis indicated that both sulfuric acid and CAM enlarged the size of aggregate particle in bauxite residue, which was conducive to improve the physical structure of substrates, accelerating the process of soil formation;
3) Pot experiment showed that the neutralized residue was suitable for the growth of ryegrass. But the accumulation of organics in plants was less than that grown on soil, indicating that organics should be introduced to bauxite residue during ecological restoration.

5. Acknowledgements

This work was supported financially by the National Key Research and Development Program of China (No. 2018YFC1901901), Natural Science Foundation of China (No. U1704252, 51704329), Key Laboratory of Hunan Province for Clean and Efficient Utilization of Strategic Calcium-containing Mineral Resources (No. 2018TP002), and Collaborative Innovation Center for Clean and Efficient utilization of Strategic Metal Mineral Resources, and Open Foundation of State Key Laboratory of Mineral Processing (No. BGRIMM-KJSKL-2019-18).

6. References

1. (a) Li Wang, Guangyan Hu, Fei Lyu, Tong Yue, Honghu Tang, Haisheng Han, Yue Yang, Runqing Liu and Wei Sun, *Minerals* 2019, vol. 9. ; (b) Li Wang, Ning Sun, Honghu Tang and Wei Sun, *Minerals* 2019, vol. 9.
2. A. Agrawal, K. K. Sahu and B. D. Pandey, *Resources, Conservation and Recycling* 2004, vol. 42, pp. 99-120.
3. Emile Mukiza, LingLing Zhang, Xiaoming Liu and Na Zhang, *Resources, Conservation and Recycling* 2019, vol. 141, pp. 187-199.
4. F. Lyu, J. D. Gao, N. Sun, R. Q. Liu, X. D. Sun, X. F. Cao, L. Wang and W. Sun, *Minerals Engineering* 2019, vol. 131, pp. 66-72.
5. J. Carneiro, D. M. Tobaldi, W. Hajjaji, M. N. Capela, R. M. Novais, M. P. Seabra and J. A. Labrincha, *Ceramics International* 2018, vol. 44, pp. 4211-4219.
6. Xiao Chen, Yugang Guo, Song Ding, Haoyu Zhang, Feiyue Xia, Jie Wang and Mingkai Zhou, *Journal of Cleaner Production* 2019, vol. 207, pp. 789-800.
7. Yanxiu Wang, Ting-an Zhang, Guozhi Lyu, Fangfang Guo, Weiguang Zhang and Yuhai Zhang, *Journal of Cleaner Production* 2018, vol. 188, pp. 456-465.
8. R. K. Paramguru, P. C. Rath and V. N. Misra, *Mineral Processing and Extractive Metallurgy Review* 2004, vol. 26, pp. 1-29.
9. X. Liu and N. Zhang, *Waste Manag Res* 2011, vol. 29, pp. 1053-63.
10. Dong-Yan Liu and Chuan-Sheng Wu, *Materials* 2012, vol. 5, pp. 1232-1246.
11. (a) J. W. C. Wong and G. E. Ho, *Waste Management & Research* 1993, vol. 11, pp. 249-256. ; (b) Shengguo Xue, Feng Zhu, Xiangfeng Kong, Chuan Wu, Ling Huang, Nan Huang and William Hartley, *Environmental Science and Pollution Research* 2016, vol. 23, pp. 1120-1132.
12. M. A. Khairul, Jafar Zanganeh and Behdad Moghtaderi, *Resources, Conservation and Recycling* 2019, vol. 141, pp. 483-498.
13. Youngjae Kim, Youngmin Lee, Minseuk Kim and Hyunsik Park, *Journal of Cleaner Production* 2019, vol. 207, pp. 490-497.
14. David Dodoo-Arhin, Rania A. Nuamah, Benjamin Agyei-Tuffour, David O. Obada and Abu Yaya, *Case Studies in Construction Materials* 2017, vol. 7, pp. 45-55.

15. I. M. Nikbin, M. Aliaghazadeh, Charkhtab Sh and A. Fathollahpour, *Journal of Cleaner Production* 2016, vol. 172, pp. 2683-2694.
16. C. V. H. Rao, N. P. Ganapati, P. V. V. Satyanayarana and S. Adiseshu, *IOSR Journal of Engineering* 2012, vol. 2, pp. 14-20.
17. Vincenzo M. Sglavo, Stefano Maurina, Alexia Conci, Antonio Salviati, Giovanni Carturan and Giorgio Cocco, *Journal of the European Ceramic Society* 2000, vol. 20, pp. 245-252.
18. (a) I. D. Pulford, J. S. J. Hargreaves, J. Ďurišová, B. Kramulova, C. Girard, M. Balakrishnan, V. S. Batra and J. L. Rico, *Journal of Environmental Management* 2012, vol. 100, pp. 59-64. ; (b) Daniel Véras Ribeiro, João António Labrincha and Marcio Raymundo Morelli, *Materials Research* 2011, vol. 14, pp. 60-66.
19. Martin Urík, Marek Bujdoš, Barbora Milová-Žiaková, Petra Mikušová, Marek Slovák and Peter Matúš, *Journal of Inorganic Biochemistry* 2015, vol. 152, pp. 154-159.
20. Xiao-bo Zhu, Wang Li and Xue-mao Guan, *Transactions of Nonferrous Metals Society of China* 2015, vol. 25, pp. 3139-3145.
21. Shrey Agrawal, Veeranjanayulu Rayapudi and Nikhil Dhawan, *Materials Today: Proceedings* 2018, vol. 5, pp. 17064-17072.
22. Bing Xue, Botao Wei, Liuxia Ruan, Fangfei Li, Yinshan Jiang, Weijun Tian, Bo Su and Liming Zhou, *Hydrometallurgy* 2019, vol. 186, pp. 91-97.
23. Kanggen Zhou, Chunying Teng, Xuekai Zhang, Changhong Peng and Wei Chen, *Hydrometallurgy* 2018, vol. 182, pp. 57-63.
24. P. James Joyce, Tobias Hertel, Andrei Goronovski, Alan H. Tkaczyk, Yiannis Pontikes and Anna Björklund, *Resources, Conservation and Recycling* 2018, vol. 138, pp. 87-98.
25. Suk-Pyo Kang and Seung-Jun Kwon, *Construction and Building Materials* 2017, vol. 133, pp. 459-467.
26. Wen-wen Zhang, Chong Wang, Rui Xue and Li-jie Wang, *Journal of Integrative Agriculture* 2019, vol. 18, pp. 1360-1368.
27. (a) Zhaobo Liu, Hongxu Li, Mengmeng Huang, Dongmin Jia and Na Zhang, *Hydrometallurgy* 2017, vol. 167, pp. 92-100. ; (b) L. V. Guozhi, Zhu Xiaofeng, Zhang Ting'an, Guo Fangfang, Pan Lu, Liu Yan, Zhao Qiuyue, Li Yan, Jiang Xiaoli and He Jicheng, In *Light Metals 2014*, ed. John Grandfield (Springer International Publishing: Cham, 2016), pp 91-95.
28. Rodolfo Marin Rivera, Brecht Ulenaers, Ghania Ounoughene, Koen Binnemans and Tom Van Gerven, *Minerals Engineering* 2018, vol. 119, pp. 82-92.
29. G. Power, M. Gräfe and C. Klauber, *Hydrometallurgy* 2011, vol. 108, pp. 33-45.